



Fragility assessment of tunnels in soft soils using artificial neural networks

Zhongkai Huang^a, Sotirios A. Argyroudis^{b,*}, Kyriazis Pitilakis^c, Dongmei Zhang^a,
Grigorios Tsinidis^c

^a Key Laboratory of Geotechnical and Underground Engineering of Ministry of Education, Department of Geotechnical Engineering, Tongji University, Shanghai, China

^b Department of Civil and Environmental Engineering, Brunel University London, Uxbridge UB8 3PH, United Kingdom

^c Department of Civil Engineering, Aristotle University, Thessaloniki, Greece

Received 24 May 2021; received in revised form 26 July 2021; accepted 30 July 2021

Abstract

Recent earthquakes have shown that tunnels are prone to damage, posing a major threat to safety and having major cascading and socioeconomic impacts. Therefore, reliable models are needed for the seismic fragility assessment of underground structures and the quantitative evaluation of expected losses. Based on previous researches, this paper presented a probabilistic framework based on an artificial neural network (ANN), aiming at the development of fragility curves for circular tunnels in soft soils. Initially, a two-dimensional incremental dynamic analysis of the nonlinear soil-tunnel system was performed to estimate the response of the tunnel under ground shaking. The effects of soil-structure-interaction and the ground motion characteristics on the seismic response and the fragility of tunnels were adequately considered within the proposed framework. An ANN was employed to develop a probabilistic seismic demand model, and its results were compared with the traditional linear regression models. Fragility curves were generated for various damage states, accounting for the associated uncertainties. The results indicate that the proposed ANN-based probabilistic framework can result in reliable fragility models, having similar capabilities as the traditional approaches, and a lower computational cost is required. The proposed fragility models can be adopted for the risk analysis of typical circular tunnel in soft soils subjected to seismic loading, and they are expected to facilitate decision-making and risk management toward more resilient transport infrastructure.

Keywords: Circular tunnels; Fragility curves; Artificial neural network; Numerical study; Probabilistic seismic demand model

1 Introduction

Tunnels play a vital role in satisfying the growing infrastructure needs around the world (Huang & Zhang, 2016; Jin et al., 2019; Zheng et al., 2021), especially in densely populated urban regions (Tsinidis et al., 2020). Therefore, seismic safety and understanding of potential induced damage are crucial in the design and rehabilitation of new and existing tunnels in earthquake prone areas. This becomes more relevant, considering the cases of reported severe

damage in tunnels during previous strong earthquakes, such as the 2008 Wenchuan (Yu et al., 2016), the 1999 Chi-Chi (Wang et al., 2021), and the 1995 Kobe events (Billings, 1995; Sayed et al., 2019), which ultimately led to significant socioeconomic losses. Hence, reliable seismic fragility and risk analysis of underground structures subjected to various earthquake scenarios becomes a critical issue for the resilience assessment of existing transport assets and networks, as well as for the design of new infrastructure.

Fragility curves, constitute a critical tool for the risk analysis of tunnels, describing the exceedance probability of different damage states (X_{DS}) against a given hazard

* Corresponding author.

E-mail address: sotirios.argyroudis@brunel.ac.uk (S.A. Argyroudis).

intensity measure (X_{IM}). Empirical fragility curves can be derived based on expert elicitations or damage evidence from past earthquake events (ALA, 2001; Corigliano et al., 2007; Ptilakis et al., 2006). Numerically derived fragility curves developed based on the framework of Performance-Based Earthquake Engineering (PBEE), constitute a current trend in the field. Recent studies proposed fragility models for circular tunnels in soft layered soils based on numerical simulations, considering representative types of soil and tunnel lining (Argyroudis & Ptilakis, 2012; Argyroudis et al., 2017; de Silva et al., 2021; Hu et al., 2020; Huang et al., 2020). However, further research is needed to improve our understanding of tunnels' seismic response and enable new approaches that allow the development of rigorous models for rapid and case-specific risk assessment of underground structures.

In most of the above numerical fragility models, a linear regression method is utilized to compute the exceedance damage probability, following a lognormal distribution (Argyroudis & Ptilakis, 2012; Argyroudis et al., 2017; Hu et al., 2020). It is assumed that the intensity measure (X_{IM}) and damage measure (X_{DM}), usually defined in terms of the tunnel lining bending moment capacity (Argyroudis & Ptilakis, 2012; de Silva et al., 2021), exhibit a linear relationship in the logarithmic space (Jalayer et al., 2015). However, this assumption may not always hold true, considering that the dynamic response history data of tunnels inherently exhibits complex and nonlinear behaviour (Chen et al., 2020). In fact, the data cloud ($\ln X_{IM}$, $\ln X_{DM}$) has the potential to follow a nonlinear form. In recent years, the development of artificial intelligence (AI) has brought new opportunities in civil engineering. Artificial neural network (ANN), which is one of the most popular machine learning algorithms (Hassoun, 1995; Zhang et al., 2021a), is often utilized to predict the performance of nonlinear systems due to its high nonlinear mapping ability. This approach can facilitate more rigorous estimations of the damage measure X_{DM} in seismic analysis of tunnels. Furthermore, the traditional seismic fragility analysis usually requires computationally demanding dynamic simulations based on finite element modelling to obtain sufficient analysis results (Shokri & Tavakoli, 2019). Properly trained and tested ANN-based models may be utilized as a fast and effective way to substitute time-consuming dynamic analyses, thus, lower computational power is required for the analyses (Lagaros et al., 2009). Recent studies have employed ANN models for the fragility assessment of reinforced concrete structures (Mitropoulou & Papadrakakis, 2011), steel structures (Liu & Zhang, 2018), nuclear power plants (Wang et al., 2018) and bridges (Mangalathu et al., 2018). It is noted that most of the existing works focus on the fragility assessment of aboveground structures, while to the best knowledge of the authors, there is no relevant research concerning underground structures.

In this respect, this paper extends the previous work by Huang et al. (2020) by applying an ANN-based methodology to evaluate the seismic fragility of circular tunnels in

soft soils. Figure 1 presents the flowchart of the proposed methodology, which will be discussed in detail in the following sections. The organization of the paper follows the flowchart. Initially, the finite element approach used to model the investigated soil-tunnel system is summarised (Section 2). The proposed numerical approach is applied to evaluate the seismic performance of the examined tunnels under increasing seismic excitation, expressed by well-defined damage measures (Section 3.1). Subsequently, an ANN model is constructed (Section 3.2) to generate the probabilistic seismic demand model (PSDM) of the studied tunnels. The advantages of the ANN model over the traditional linear regression method are discussed. Furthermore, the correlation of five different widely used intensity measures (X_{IM}) with the seismic response of the studied tunnels is also discussed (Section 3.3), aiming at the definition of the most efficient X_{IM} . The examined X_{IM} includes the peak ground acceleration (a_{PG}), the peak ground velocity (V_{PG}), the peak ground displacement (D_{PG}), the ratio between V_{PG} and a_{PG} , i.e., $F_{r1} = V_{PG}/a_{PG}$, and the Arias intensity (I_a). Finally, based on the proposed ANN-based PSDM and the derived efficient IM , i.e., V_{PG} , fragility curves are established for the examined soil-tunnel configurations (Sections 3.4 and 4). These curves are compared with the ones developed based on traditional linear regression method (Sections 4 and 5).

2 Conceptual assumptions and analysis of soil-tunnel configurations

2.1 Tunnel and soil parameters

A circular tunnel section with an external diameter d of 6.2 m representative of the Shanghai metro network is chosen as a studied case. The thickness of the tunnel lining is 0.35 m and the concrete cover depth of the lining is 50 mm. The burial depth C from the ground surface to the top of the tunnel is 20 m, corresponding to a moderately deep tunnel section. The elastic modulus E_c and Poisson's ratio ν_c of reinforced-concrete tunnel are 3.55 GPa and 0.2, respectively.

Two soil profiles with clayey and sandy layers, corresponding to typical soft soil conditions in Shanghai, are considered in this study. The layered soil profiles, denoted as IV-1 and IV-2, are categorized as ground type IV based on the Chinese seismic code (GB50011—2010). The detailed geotechnical properties of soils and the shear wave velocities profiles as well as the variations of normalized shear stiffness G/G_{max} and damping ratio D_r with shear strain γ for the examined sites can be further referenced from author's previous work (Huang et al., 2021).

2.2 Development of the soil-tunnel numerical model

Since the transversal response of the tunnels under ground shaking is more critical than the longitudinal one, i.e., higher potential for damage during shaking in

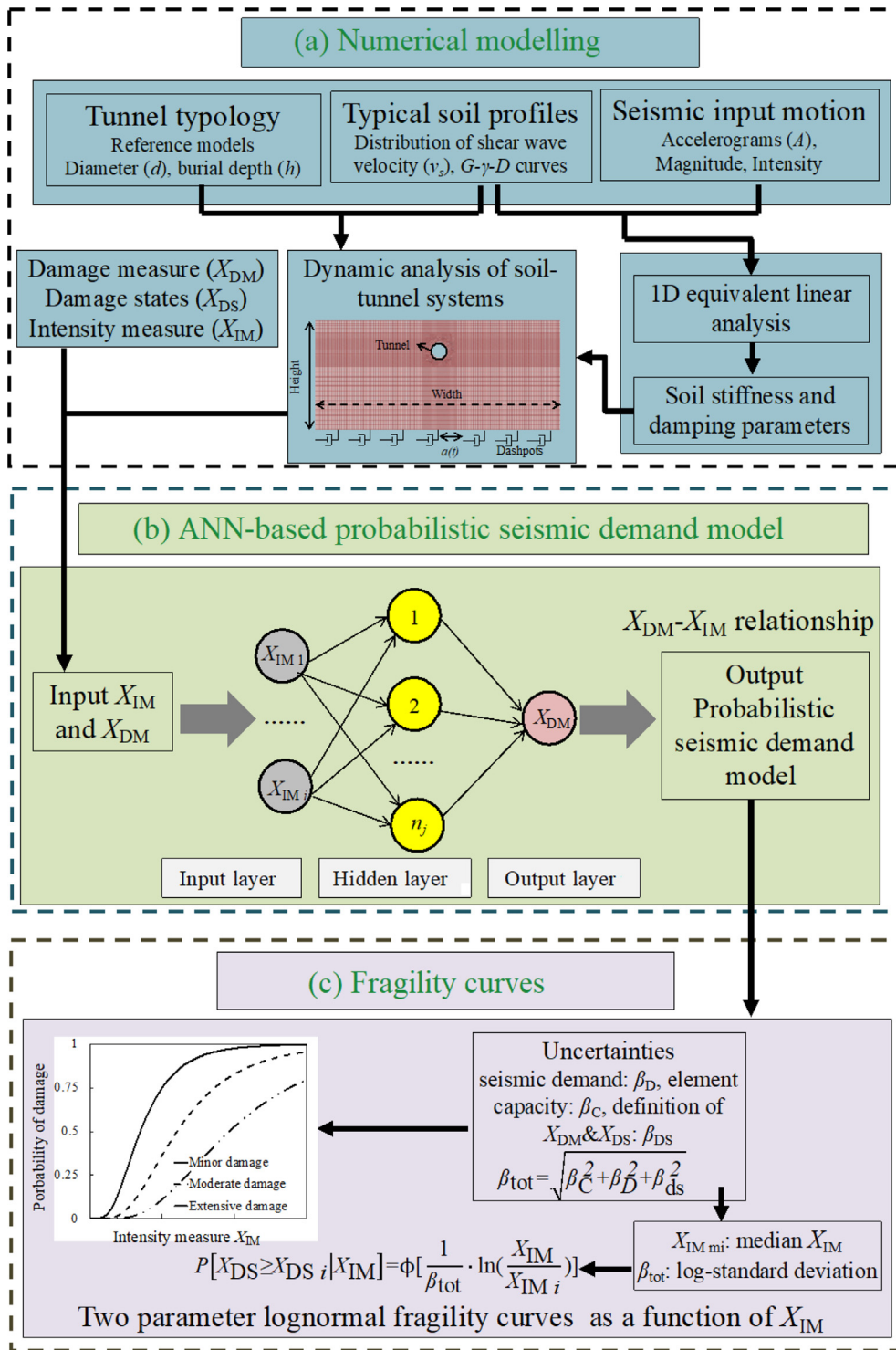


Fig. 1. Probabilistic framework for seismic fragility assessment of tunnels using artificial neural network (ANN).

transversal direction (Hashash et al., 2001; Tsinidis et al., 2020), this study is focused in 2D conditions. Moreover, the seismic response of the examined tunnel is considered only in circumferential conditions; hence, it can be seen

as a plane strain problem. In this respect, the potential 3D effects are ignored for simplicity, and a two-dimensional model of the soil-tunnel system is generated using ABAQUS (2011), as shown in Fig. 2. The model

domain is 400 m wide and 100 m deep, the ground beyond this depth is assumed to be ‘elastic bedrock’ for the studied soil profiles. Two-node beam elements (B21) are used to model the tunnel lining. The interaction between tunnel-soil interface is simulated by a finite-sliding hard contact model. The normal interface behavior is controlled through a hard contact formulation, while the tangential interface behavior is modelled through a Coulomb frictional model. A friction coefficient $\mu = 0.6$ is used for the tunnel-soil interface. The soil is simulated by the plane strain elements (CPE4R). The mesh size is properly chosen based the rule proposed by [Lysmer and Kuhlemeyer \(1969\)](#). Moreover, a finer discretization is adopted for the surrounding soil elements close to the lining, ensuring the efficient simulation of the soil-tunnel interaction effects.

The elastic bedrock is modelled using the dashpots, to minimize seismic wave reflections ([Lysmer & Kuhlemeyer, 1969](#)). Horizontal kinematic tie constraints are introduced for the nodes on the side boundaries of the model, to ensure that the opposite vertical sides have the same movement, following [Tsinidis et al. \(2014\)](#).

The tunnel lining is simulated utilizing a linear elastic model, while the behaviour of the soil is modelled by a visco-elasto-plastic model with a Mohr–Coulomb yield criterion. Soil parameters are calibrated following [Tsinidis et al. \(2015, 2016\)](#) based on 1D soil response analysis with EERA ([Bardet et al., 2000](#)). The viscous damping of the soil is introduced in the analysis in the form of Rayleigh damping, calibrated properly for critical frequencies of the system. The other simulation procedure and numerical modelling is described in more detail in authors’ previous work ([Huang et al., 2021](#)).

The proposed numerical modelling approach is used to calculate the seismic response of tunnel and generate the database for the fragility analysis. The proposed numerical model has some limitations. For instance, the volume loss is not considered in this study. Generally, as we can expect, the excavation process may alter to some extent the initial state of stress close to the tunnel. Since the study mainly focuses on the dynamic soil inelastic response, the tunnel

is simulated as being in place within a geostatic step, producing a reasonable “reference” initial stress state around the tunnel. This modelling procedure has been widely adopted by other researchers (e.g., [Hatzigeorgiou & Beskos, 2010](#); [de Silva et al., 2021](#)). Moreover, the cumulative shaking effects are ignored since this study focuses on the vulnerability of tunnels in the case of a single strong seismic event, which is in line with previous studies (e.g., [Nguyen et al., 2019](#); [de Silva et al., 2021](#); [Zi et al., 2021](#)). The above limitations, as well as some additional issues, e.g., the implementation of more advanced soil constitutive models are issues to be examined in future studies.

2.3 Input ground motion characteristics

The selection of earthquake motions is of prior importance for the seismic fragility analysis. [Liu et al. \(2017\)](#) reported that a suite of 10–20 well-chosen earthquake records can meet the needs for the accurate computation of seismic demands of studied structures. Twelve different records are selected in the framework of this study ([Table 1](#)). The selection is made from the [PEER \(2000\)](#) strong motion database, following the commonly used spectral matching method ([Gardoni et al., 2003](#); [Iervolino & Manfredi, 2008](#)). The acceleration response spectra of the selected records compare well with the design response spectrum from the Chinese seismic code ([GB50011—2010](#)). More details of this comparison and the selection of earthquake motions were provided by [Huang et al. \(2021\)](#). In this work, the incremental dynamic analysis ([Vamvatsikos & Cornell, 2002](#)) was adopted to cover a wider range of ground motion amplitudes. To evaluate the seismic response of tunnel lining under an increasing increment of seismic intensity, the peak of the selected earthquake motions was scaled from 0.1 g to 1.0 g with a step of 0.1 g. This is a common approach in similar studies related to the fragility assessment of structures ([de Silva et al., 2021](#); [Nguyen et al., 2019](#); [Zhong et al., 2020](#)). Thus, a total of 120 input motions are finally used to develop the fragility curves.

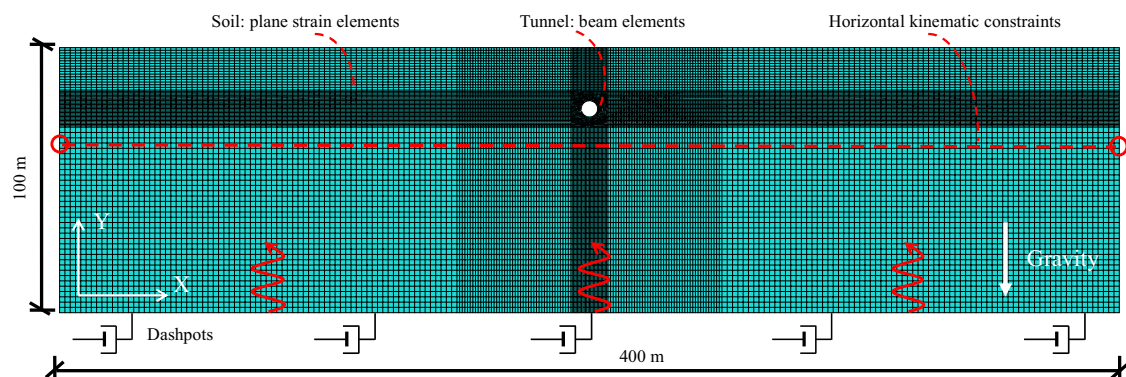


Fig. 2. Finite element soil-structure-interaction (SSI) model for the soil-tunnel system.

Table 1
Properties of the selected records.

Earthquake	Station name	Year	Mag. (M_w)	R (km)	a_{PG} (g)
Kobe, Japan	Port Island	1995	6.90	3.31	0.32
Northridge USA	LA - Hollywood Stor FF	1994	6.69	19.73	0.23
Parkfield, USA	Cholame-Shandon Array	1966	6.19	12.90	0.24
Imperial Valley-07, USA	El Centro Array #11	1979	5.01	13.61	0.19
Superstition Hills-01, USA	Imperial Valley W.L. Array	1987	6.22	17.59	0.13
San Fernando, USA	Castaic - Old Ridge Route	1971	6.61	19.33	0.34
Tottori, Japan	TTR008	2000	6.61	6.86	0.39
Parkfield-02, USA	Parkfield-Cholame 2WA	2004	6.00	1.63	0.62
Borrego Mtn, USA	El Centro Array #9	1968	6.63	45.12	0.16
Loma Prieta, USA	Treasure Island	1989	6.93	77.32	0.16
Kern County, USA	Taft Lincoln School	1952	7.36	38.42	0.15
Imperial Valley-02, USA	El Centro Array #9	1940	6.95	6.09	0.28

Notes: R is epicentral distance, Mag. is moment magnitude, and a_{PG} is peak ground acceleration.

3 Development of PSDM

3.1 Definition of damage measure and damage states

The definitions of the damage measure (X_{DM}) and damage states (X_{DS}), constitute critical components for the fragility analysis of any element at risk, as they should directly reflect the seismic response of the examined element (Argyroudis et al., 2019). In this study, five damage states are defined in terms of the ratio of the actual bending moment (M_{Sd}) over the capacity bending moment (M_{Rd}) of the tunnel cross-section, describing the exceedance of none, minor, moderate, extensive and complete damage of the tunnel lining. The limit values for different damage states are defined based on available literature (Argyroudis & Pitilakis, 2012), as shown in Table 2. The proposed damage measure and damage states have been used in similar studies (e.g., Hu et al., 2020; de Silva et al., 2021). Herein, the actual bending moment of the tunnel lining is evaluated through the dynamic analyses, while the capacity of bending moment is computed by a section analysis using the lining geometry and material properties.

3.2 ANN-based probabilistic seismic demand model

An ANN is used to generate the PSDM of the studied configurations, accounting for the capability of the method to deal with nonlinear regression issues, with good prediction performance and without time consuming numerical

simulations. The application of an ANN can effectively reveal complex nonlinearities, which inherently exist among the structural response data obtained from incremental dynamic analysis, and ultimately result in more precise and reliable estimations of damage measure (X_{DM}) for the studied tunnels. Figure 3 shows the typical structure of the ANN model used in this work, which generally contains six basic elements, i.e., (i) the input layer, (ii) the output layer, (iii) the hidden layer, (iv) the connection weights between each layer, (v) the bias parameter associated with each neuron in the hidden layer and (vi) the activation functions. The input layer receives the information from the input neurons and transforms such information to the hidden layer, which is located between the input and output layers. The hidden layer plays a role in applying the transformation from the input layer to the output layer. The output layer represents the solution of the model, i.e., the damage measure in this study. The weights are adjusted to connect the neurons in the different layers, and the bias parameter is set to avoid the model output null values by zero inputs. The activation functions are used to establish the non-linear correlations between input and output neurons. In this study, X_{IM} and the structural damage measure are set as the input and output of the model, respectively.

The ANN model in this study was established according to the multilayer perceptron (MLP), trained by the algorithm called as feed-forward back-propagation (BPP). Specifically, the ANN model was trained by the Levenberg-Marquardt back-propagation algorithm

Table 2
Adopted damage measure and damages states (Argyroudis & Pitilakis, 2012).

Damage state (X_{DS})	Range of damage measure (X_{DM})	Central value of X_{DM}
X_{DS0} : none	$M_{Sd}/M_{Rd} \leq 1.0$	—
X_{DS1} : minor	$1.0 < M_{Sd}/M_{Rd} \leq 1.5$	1.25
X_{DS2} : moderate	$1.5 < M_{Sd}/M_{Rd} \leq 2.5$	2.00
X_{DS3} : extensive	$2.5 < M_{Sd}/M_{Rd} \leq 3.5$	3.00
X_{DS4} : complete	$M_{Sd}/M_{Rd} \geq 3.5$	—

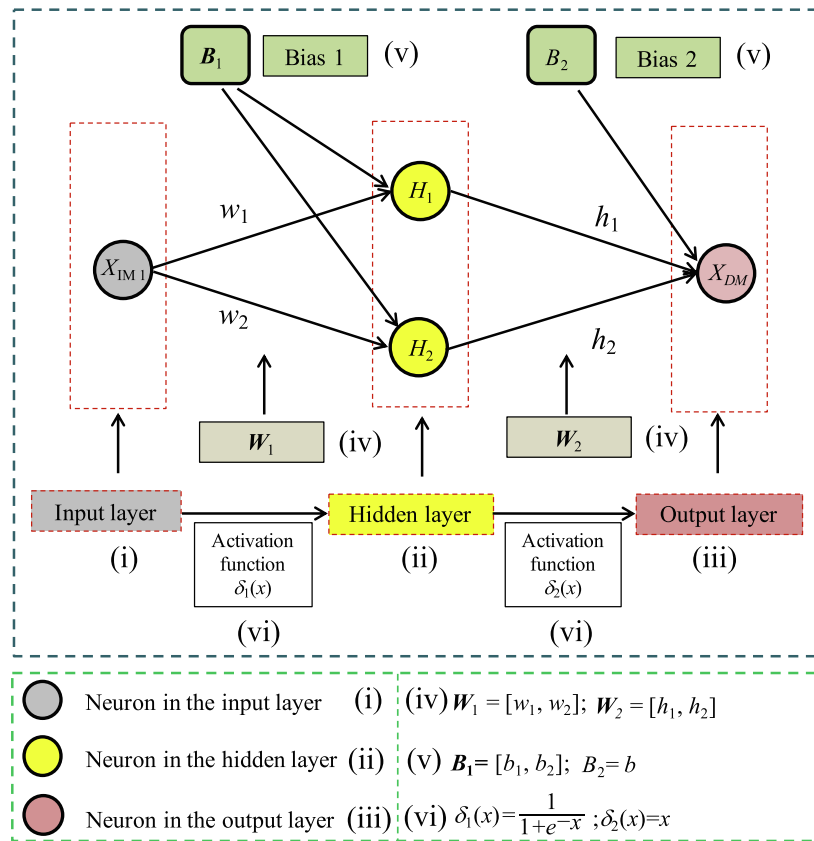


Fig. 3. ANN-based PSDM.

(Marquardt, 1963) provided by MATLAB (2018), to calculate the associated weights and biases between different layers. The above calculated datasets (i.e., X_{IM} - X_{DM} data pairs) were randomly divided into training and testing sets, respectively. Specifically, 80% of datasets were utilized for training, and the remaining random 20% of data were used for testing process. It is noted that the data division (i.e., 80/20 percent) adopted in this study is commonly used by other researchers (e.g., Ranasinghe et al., 2017; Zhang et al., 2021b; Chen et al., 2021) in similar research topics. This data division method can guarantee sufficient dataset to test the accuracy of ANN. Meanwhile, the dataset of training was used to calculate the biases and connection weights in different layers, while the dataset of testing was utilized to measure the performance of the ANN model and guarantee that the overfitting problems do not happen in the ANN model.

Considering that the interval of the input and output parameters are different to the same scale, the input and output parameters of the ANN model were scaled in a range of -1 and 1 based on Eq. (1), to achieve dimensional consistency of all the parameters. Moreover, with this normalization, the ANN has a better convergence performance during the training process, and potential overfitting issues are avoided.

$$Y_n = 2 \times \frac{(Y_i - Y_{\min})}{(Y_{\max} - Y_{\min})} - 1, \quad (1)$$

where Y_n is the normalized parameter, Y_i is the corresponding data to be normalized, and Y_{\max} and Y_{\min} stand for the maximum and minimum data of the considered parameter, respectively.

For simplicity, only one hidden layer was used in the ANN model of this study, as previous studies (Chern et al., 2009; Salsani et al., 2014) have indicated that the ANN model with one hidden layer can have a rather excellent performance in similar problems. Hence, the final ANN consists of one hidden layer and one output layer. Moreover, in the hidden layers, the logistic sigmoid (LOG-SIG) nonlinear function of $\delta(x) = \frac{1}{1+e^{-x}}$ is used as an activation function of the neurons, while in the output layers, the pure linear (PURELIN) activation function of $\delta(x) = x$ is utilized. Their functions are presented in Fig. 4. The above two activation functions are widely applied in the field of civil engineering (Liu & Zhang, 2018; Mangalathu et al., 2018). Levenberg-Marquardt (LM) learning algorithm (Khosravikia et al., 2020; Shahin et al., 2001) is adopted in this study to train the network and calculate the corresponding connection weights and bias terms.

The number of neurons in the hidden layer is determined through the trial-and-error method, and the mean square error (MSE) is used to assess their performance. Figure 5 presents the calculated MSE values for various neurons ranging from one to six using the data pairs of V_{PG} and X_{DM} . It is obvious that the maximum MSE is

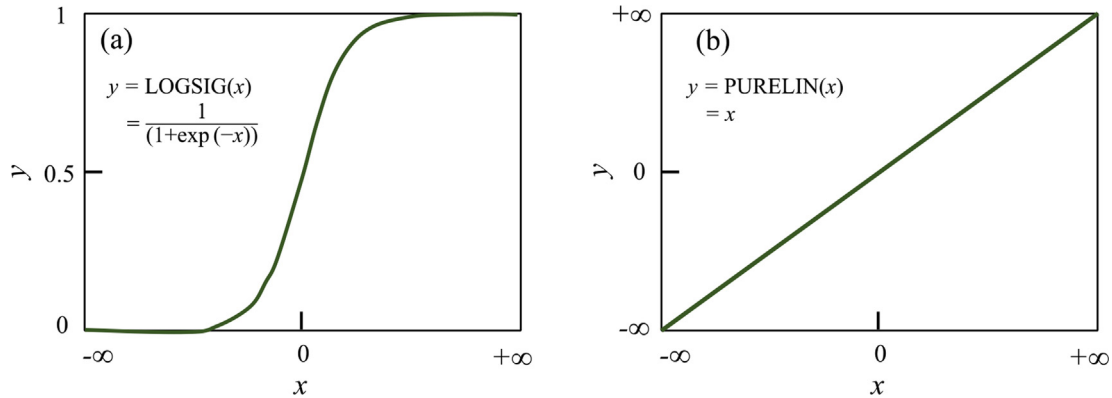


Fig. 4. Activation functions: (a) LOGSIG and (b) PURELIN.

observed when the number of neurons is one, while the minimum MSE is found when the number of neurons is six. Generally, the value of MSE is quite similar when the number of neurons is larger than one, and the results indicate that the reduction of MSE is not significant when the number of neurons in the hidden layer range between two and six. Similar conclusions can be obtained for the other data pairs of considered X_{IM} and X_{DM} . The quick convergence of the ANN may be attributed to the nature of the examined problem, i.e., only one input parameter and one output parameter are examined in the problem in hand. The trend between the input and output parameter is easy to be captured by ANN model with a small number of neurons in the hidden layer. It is noted that if multiple-input and output parameters exist, it is more difficult to achieve convergence of ANN compared to the case in this study (Haykin, 2010). Additionally, as addressed by Lagaros et al. (2009), utilizing three or more neurons, in which the output (X_{DM}) is predicted via only one input (X_{IM}), may result in adverse overfitting issues. Hence, for the sake of simplicity, two neurons are selected for the hidden layer of the proposed ANN model.

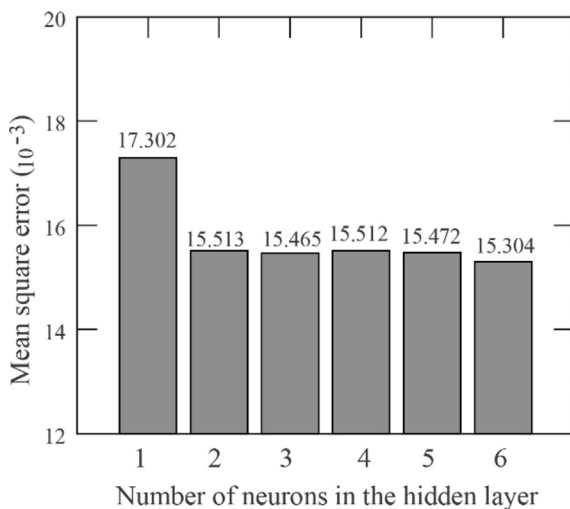


Fig. 5. Performance of different number of neurons in the hidden layer (case: V_{PG} and X_{DM}).

After training, using the connecting weights and biases as well as the transfer function, an ANN network shown in Fig. 3 can be described by Eq. (2):

$$X_{DM} = b + \sum_{i=1}^2 h_i \times \left[\frac{1}{1 + \exp[-(w_i \times (X_{IM}) + b_i)]} \right], \quad (2)$$

where b and b_i are the bias at the output layer and the i -th neuron of the hidden layer, respectively; h_i is the connection weight between the i -th neuron of the hidden layer and the output neuron; w_i is the connection weight between the input layer and i -th neuron of the hidden layer. The connection weights and bias values can be calculated during the training process. Using Eq. (2) and the corresponding coefficients, the XDM of the studied tunnels can be easily estimated for a given X_{IM} of the ground motion without re-training the ANN model.

3.3 Selection of efficient seismic intensity measure

The potential correlations of different seismic X_{IM} with the seismic response of the tunnel are briefly discussed in this section aiming at selecting the most efficient one within the proposed fragility assessment framework. The examined X_{IM} includes the peak ground acceleration (a_{PG}), the peak ground velocity (V_{PG}), the peak ground displacement (D_{PG}), the ratio between V_{PG} and a_{PG} , i.e., $F_{r1} = V_{PG}/a_{PG}$, and the Arias intensity (I_a). In this context, these X_{IM} are set separately as input of the proposed ANN model shown in Fig. 3, to obtain the corresponding PSDM. Generally, an efficient X_{IM} should result in a relatively low dispersion in the seismic response of examined structures and thus more reliable results of the fragility assessment (Karafagka et al., 2021). A term, defined as $\beta_{DM/IM}$, is adopted as the metric to represent the efficiency of each X_{IM} . Herein, $\beta_{DM/IM}$ is computed by conducting statistical processing of the numerical results ($\ln X_{IM}$ - $\ln X_{DM}$ data pairs). More specifically, $\beta_{DM/IM}$ is estimated as the dispersion of the simulated X_{DM} regarding the regression fit for the corresponding numerical data using the following equation:

$$\beta_{DM/IM} = \sqrt{\frac{\sum_{i=1}^N [\ln(X_{DMi}) - \ln(X_{DM})]^2}{N-2}}, \quad (3)$$

where X_{DMi} is the calculated damage measure and N is the total number of dynamic nonlinear analyses of the studied tunnels.

The 240 X_{IM} - X_{DM} data pairs derived from 2D numerical analyses are utilized in the development and the training of the ANN-based model for the five selected X_{IM} . Figure 6 summarizes the dispersions, $\beta_{DM/IM}$, between the predictions of the damage measure X_{DM} of the studied tunnel and five X_{IM} . The results indicate a significantly lower dispersion, i.e., 0.13, when V_{PG} is used as X_{IM} compared to the other four X_{IM} , indicating that V_{PG} is the most 'efficient' X_{IM} among the tested X_{IM} . This finding is well in line with the authors' previous work (Huang et al., 2021) for the same case of moderately deep tunnel and is also consistent with other studies (Corigliano et al., 2007; Chen & Wei, 2013). The potential reason for this phenomenon is that the imposed ground deformations during shaking are prevailing in dominating the seismic performance of underground structures such as tunnels in this study, and V_{PG} is a better indicator for ground deformations (γ_{max}) induced during ground shaking, as mentioned in NCHRP 611 report (Anderson et al., 2008) and Ptilakis and Tsinidis (2014). Hence, V_{PG} is better correlated with structural damage and exhibits smaller dispersion in Fig. 6, compared to other studied X_{IM} . Furthermore, D_{PG} and I_a have a similar dispersion of about 0.25, while F_{R1} is the least 'efficient' X_{IM} as it has the highest dispersion of 0.37 among the five tested X_{IM} . In other words, V_{PG} produces the best prediction of the damage measure X_{DM} of the tunnels. Therefore, the use of V_{PG} as the X_{IM} for the construction of fragility curves is suggested in this study, considering that the total dispersion is lower. Hence, it is expected that the assessment of the probabilities of exceeding various damage states will be more accurate. In this

regard, Table 3 presents the connection weights and bias values of the trained ANN for the development of PSDM of the studied tunnel by using V_{PG} as the X_{IM} .

3.4 Comparison of ANN-based PSDM with traditional linear models

In this section, the prediction capabilities of the ANN-based and traditional linear-based PSDM are compared by using V_{PG} as the X_{IM} . Figure 7(a) portrays pairs of damage measure X_{DM} - V_{PG} in log-log space (Huang et al., 2020), with the damage measure values being computed by the ANN model. The figure presents the line of linear regression between the damage measure and the intensity measure (black solid line). This figure indicates that the intensity measure V_{PG} and the damage measure X_{DM} do not show a perfect linear relationship in log-log space, especially for the X_{IM} - X_{DM} pairs at low V_{PG} levels. Moreover, the predictions from ANN models and linear regression are quite similar when the $\ln(X_{IM}) - \ln(X_{DM})$ pairs exhibit a linear relationship. It is clearly observed that the linear regression method does not predict data as accurately as the ANN model does. ANN is capable to correctly describe the trends inherently existed in the data sets, and outcomes more precise predictions of the damage measure X_{DM} of the studied tunnels. The standard deviations $\beta_{DM/IM}$ estimated by both methods are also computed and compared in Fig. 7(a). As shown in this figure, the implementation of the ANN method results in slightly lower deviation compared to the linear regression method.

To further examine the efficiency of the employed ANN model, in Fig. 7(b) we plotted the damage measure X_{DM} values computed by the traditional numerical analyses against the predicted values from ANN model and those of the linear regression analysis. It is observed that the data from the ANN model are closer to the 1:1 line, highlighting a better correlation between the measured and predicted data values. A higher coefficient of determination R^2 is computed by a relevant regression of data for the ANN model compared to the linear regression analysis, as shown in Fig. 7(b). Therefore, the ANN may be safely utilized to capture the PSDM for the fragility analysis of the examined tunnel as described in the following section. It should be noted that the validity of the ANN model is limited by the range of the training data (Lagaros et al., 2009). Hence, the input parameter needs to be restricted between the minimum and maximum values of the training data, i.e., 0.068 to 2.510 m/s for V_{PG} and 0.458 to 3.294 for X_{DM} . Generally, the performance and the reliability of the ANN model are better when no extrapolation is done beyond this range, and a wider range of datasets are used. Moreover, for more complex and nonlinear soil-underground structures problems, it is recommended that the above ANN-based methodology can be utilized to substitute time consuming dynamic analyses, so as to increase the computing efficiency significantly.

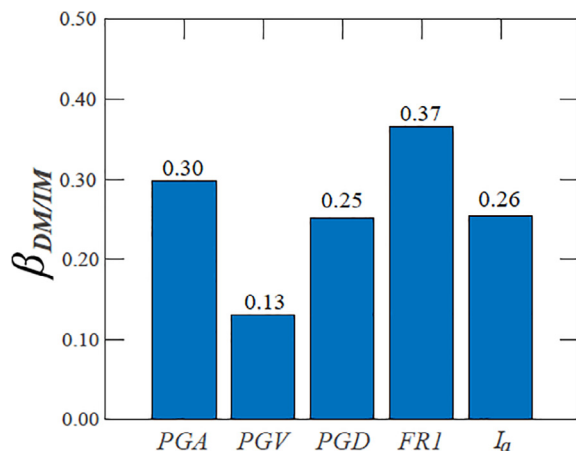


Fig. 6. Dispersion $\beta_{DM/IM}$ of results with different X_{IM} .

Table 3

Coefficients of the ANN equation for estimating damage measure X_{DM} of studied tunnels with respect to V_{PG}

X_{IM}	w_1	w_2	b_1	b_2	h_1	h_2	b	$\beta_{DM/IM}$
V_{PG}	-78.11	75.91	-0.840	-0.903	-1.928	-1.950	1.417	0.13

4 Development of fragility curves

A lognormal probability distribution function is commonly used to develop fragility curves:

$$P\left[X_{DS} \geq \frac{X_{DSi}}{X_{IM}}\right] = \phi\left[\frac{\ln(X_{IM}) - \ln(X_{IMi})}{\beta_{tot}}\right], \quad (4)$$

where $P(X_{DS} \geq X_{DSi}/X_{IM})$ is the exceeding probability for a particular damage state X_{DS} , given a seismic intensity level X_{IM} , X_{DSi} is the damage limit state, ϕ is the standard normal cumulative distribution function, X_{IMi} is the median threshold value of X_{IM} that causes a particular X_{DS}

and β_{tot} is the lognormal standard deviation representing the total dispersion related to each fragility curve. The capacity of the tunnel lining (β_C), the seismic demand ($\beta_{DM/IM}$) and the definition of damage state (β_{ds}) are the major variability dispersions for the definition of β_{tot} , as presented in Eq. (5):

$$\beta_{tot} = \sqrt{\beta_C^2 + \beta_{DM/IM}^2 + \beta_{ds}^2}. \quad (5)$$

In this study, the parameters β_{ds} and β_C are taken as 0.4 and 0.3, respectively (Argyroudis & Pitilakis, 2012; Argyroudis et al., 2013), while the parameter $\beta_{DM/IM}$ is computed by conducting statistical processing of the numerical results (i.e., $\ln X_{IM}$ - $\ln X_{DM}$ data pairs) (see Sections 3.3 and 3.4).

Using the derived PSDM in Section 3.4, the thresholds of each damage state in Table 2 and the definition of β_{tot} in Eq. (5), the two critical parameters for the development of the fragility functions, i.e., the median X_{IMi} (V_{PG}) and standard deviations β_{tot} are estimated for the examined configurations and various damage states (see Table 4).

Figure 8 shows the comparisons of the computed sets of ANN-based and linear-based analytical fragility curves for the studied tunnels in terms of V_{PG} at the ground surface in free-field conditions. It is noted that a higher β_{tot} value leads to a flatter fragility curve and thus to higher uncertainty. The herein computed β_{tot} values for the ANN-based fragility curves are lower than the ones for the linear regression analysis. Additionally, as expected, for both the ANN-based and linear-based fragility curves, the probability of damage increases as the value of V_{PG} increases for all the damages states. Moreover, for the same value of V_{PG} , it is noted that the probability of damage from ANN-based curves is very close to the one from linear-based curves for all damage states. For example, when the V_{PG} value equals to 0.55 m/s, the probabilities of exceeding minor, moderate and extensive damage for the linear-based curves are equal to 49.8%, 7.7% and 4.0%, respectively, while for the ANN-based fragility curves, they are equal to 45.6%, 9.0% and 3.0%, respectively. Generally, the above results indicate that for this level of seismic intensity, the studied tunnels are expected to suffer no damage or minor damage to some extent, so the potential to suffer extensive damage

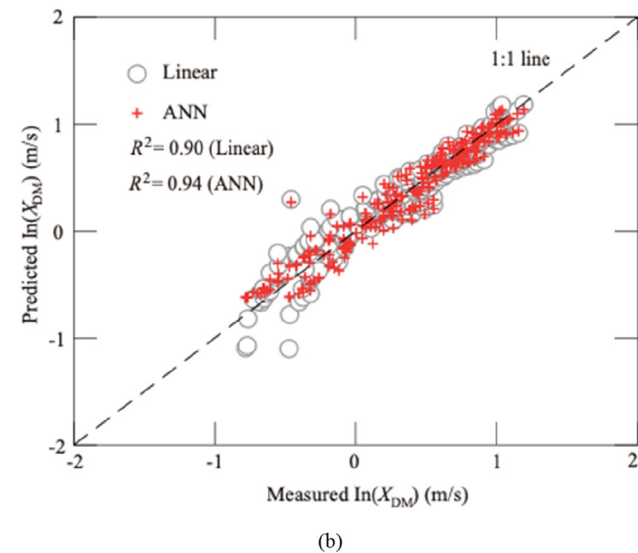
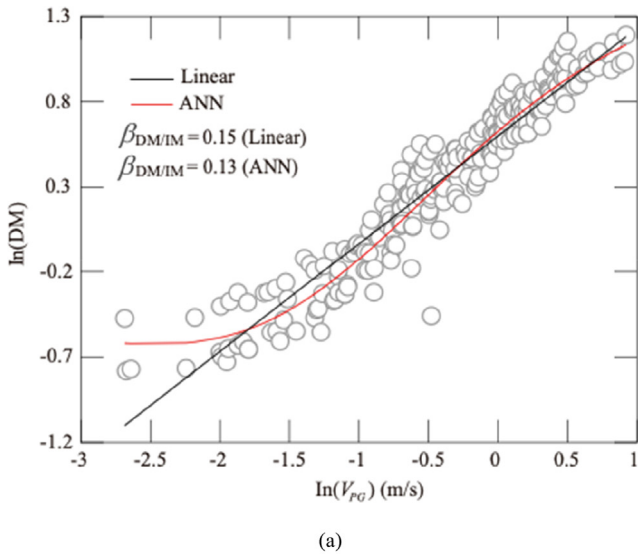


Fig. 7. Comparison between the ANN-based and linear-based PSDM: (a) $\ln(X_{DM})$ versus $\ln(V_{PG})$; (b) Predicted versus measured $\ln(X_{DM})$ values.

Table 4

Computed parameters of the fragility curves in terms of V_{PG} for the studied tunnel using ANN and linear regression analysis methods

Damage states	Minor	Moderate	Extensive	β_{tot}
	median V_{PG} (m/s)			
ANN	0.583	1.102	2.303	0.517
Linear regression analysis	0.552	1.159	2.199	0.521

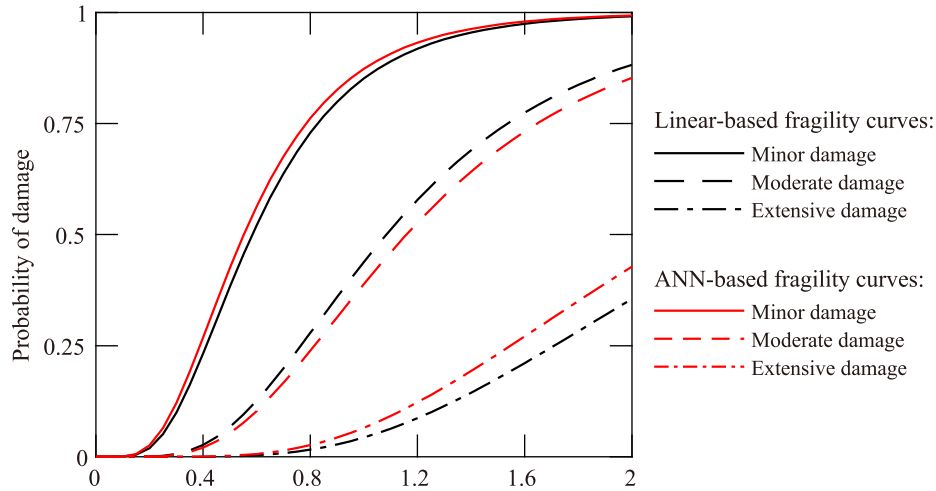


Fig. 8. Comparison of the ANN-based and linear-based fragility curves.

is negligible. The above discussion indicates that the derived vulnerability from ANN-based curves is generally close to the one from linear-based curves with slightly less uncertainty. The differences between these two approaches are really minimum and insignificant in practice. Therefore, it is concluded that the proposed ANN-based probabilistic framework for seismic vulnerability assessment of tunnels provides similar capabilities as the traditional linear regression method, but has the major advantage of significantly lower computational cost to run the whole analysis. Thus, it might be very promising for the estimation of fragility curves in case of complex soil-tunnel typologies. Moreover, the alternative use of ANN might be the key for the development of more completed analysis cases, in the sense of covering a larger cluster of tunnels and soil conditions and considering also other important parameters like aging effects.

5 Discussion

This section provides further insights into the derived fragility curves by discussing how the fragility assessments might be affected when different intensity measures are enabled, i.e., V_{PG} at the bedrock and F_{r1} at the ground surface, which is the less efficient X_{IM} (see Section 3.3).

Figure 9 shows the derived fragility curves along with their fragility parameters (median X_{IM_i} and standard deviations β_{tot}) in terms of V_{PG} at the bedrock. Naturally, the probability of damage increases gradually as the value of V_{PG} at the bedrock increases for all the damage states. Compared with the fragility curves in terms of V_{PG} at the ground surface given in Fig. 8, it is noted that a reduction of the fragility median value appears for minor damage state, while an increase of the fragility median value appears for moderate and extensive damage states.

Figure 10 shows the derived fragility curves along with their fragility parameters in terms of F_{r1} at the ground surface. As expected, the probability of damage also increases as the value of F_{r1} at the ground surface increases for all

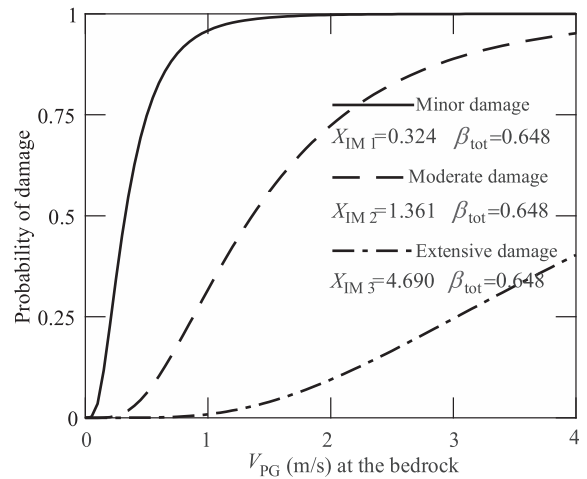


Fig. 9. Fragility curves in terms of V_{PG} at the bedrock.

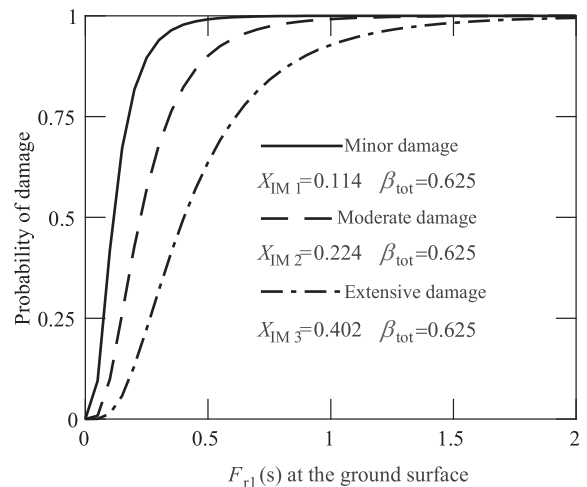


Fig. 10. Fragility curves in terms of F_{r1} at the ground surface.

damage states. It is noted that the total standard deviation β_{tot} (a value of 0.625) in Fig. 10 is generally higher than the one (a value of 0.517) in Fig. 8 in terms of V_{PG} at the

ground surface (i.e. the most efficient X_{IM}). This comparison qualitatively illustrates the way that the dispersion difference propagates to the output fragility curves between the less and most efficient X_{IM} , i.e., F_{r1} and V_{PG} at the ground surface.

6 Summary and conclusions

This study presented an artificial neural network (ANN) based probabilistic framework to assess the seismic fragility of tunnels in soft soils. The first step of the methodology included the analysis of the response of a typical circular tunnel under a variety of seismic motions, by employing 2D finite element numerical models of the examined tunnel-soil configurations. The damage measure was defined in terms of a ratio between the acting bending moment on the tunnel and the lining bending moment capacity. An ANN was utilized to generate the PSDM for the studied tunnel. V_{PG} was proved to be the most adequate intensity measure (X_{IM}) among the five tested X_{IM} (a_{PG} , V_{PG} , D_{PG} , F_{r1} , and I_a), and used to generate the seismic fragility curves. Fragility curves were derived for increasing levels of V_{PG} at the ground free-field conditions considering the various uncertainties involved. The results indicate that the proposed ANN-based probabilistic framework has similar capabilities with the traditional linear regression method. Another two sets of fragility curves in terms of V_{PG} at the bedrock and F_{r1} (i.e., the less efficient X_{IM}) at the ground surface were also presented to provide insight on how the parameters of the fragility functions and thus the loss assessment of tunnels, could be affected by the use of different X_{IM} .

The results show that once the ANN model is well trained, it can be adopted to replace time-consuming finite element modelling and conduct a large number of simulations for fragility analyses in few minutes, at negligible computational cost. Hence, the computational demand is significantly reduced compared to the traditional methods used by previous researchers (Huang et al., 2020; Liu et al., 2017; Nguyen et al., 2019). In this respect, the proposed ANN-based methodology can be also applied in the fragility analysis of more complex underground systems. To enhance the capability and accuracy of the ANN model for more complex underground systems, further investigations should be conducted for the application of other advanced machine learning algorithms such as convolutional neural network (CNN), recurrent neural network (RNN) and long-short term memory (LSTM) network.

The developed fragility curves can be used for the quantitative seismic risk and resilience analysis of circular tunnels embedded in similar soil deposits. The proposed ANN-based methodology can be further applied to establish the multivariate PSDMs that consider multiple X_{DM} in a single model, which could potentially capture better the correlation among different X_{DM} and X_{IM} , leading to more

realistic demand models and finally to more reliable fragility assessments.

Acknowledgements

This work was financially supported by National Natural Science Foundation of China (Grant Nos. 52108381, 52090082, 41772295, 51978517), Innovation Program of Shanghai Municipal Education Commission (Grant No. 2019-01-07-00-07-456 E00051) and key innovation team program of innovation talents promotion plan by MOST of China (No. 2016RA4059).

Declaration of competing interest

We know of no conflicts of interest associated with this publication, and there has been no personal relationships or significant financial support for this work that could have influenced its outcome.

References

- Abaqus (2011). *Abaqus 6.11*. Dassault Systemes Simulia Corporation, Providence, RI, USA.
- ALA (American Lifelines Alliance) (2001). *Seismic fragility formulation for water systems, Part 1*. Reston, VA, USA: American Society of Civil Engineers (ASCE)–Federal Emergency Management Agency (FEMA).
- Anderson, D. G., Martin, G. R., Lam, I., & Wang, J. N. (2008). *Seismic analysis and design of retaining walls, buried structures, slopes, and embankments* (Vol. 611). Transportation Research Board.
- Argyroudis, S. A., & Pitilakis, K. D. (2012). Seismic fragility curves of shallow tunnels in alluvial deposits. *Soil Dynamics and Earthquake Engineering*, 35, 1–12.
- Argyroudis, S. A., Mitoulis, S., Winter, M. G., & Kaynia, A. M. (2019). Fragility of transport assets exposed to multiple hazards: State-of-the-art review toward infrastructural resilience. *Reliability Engineering & System Safety*, 191, 106567.
- Argyroudis, S., Kaynia, A. M., & Pitilakis, K. (2013). Development of fragility functions for geotechnical constructions: Application to cantilever retaining walls. *Soil Dynamics and Earthquake Engineering*, 50, 106–116.
- Argyroudis, S., Tsinidis, G., Gatti, F., & Pitilakis, K. (2017). Effects of SSI and lining corrosion on the seismic vulnerability of shallow circular tunnels. *Soil Dynamics and Earthquake Engineering*, 98, 244–256.
- Bardet, J. P., Ichii, K., & Lin, C. H. (2000). *EERA: A computer program for equivalent-linear earthquake site response analyses of layered soil deposits*. Department of Civil Engineering: University of Southern California.
- Billings, I. J. (1995). Restoration of road and rail transportation following the Great Hanshin Earthquake of 17 January 1995. *Bulletin of the New Zealand Society for Earthquake Engineering*, 28(4), 311–334.
- Chen, J., Zhou, M., Huang, H., Zhang, D., & Peng, Z. (2021). Automated extraction and evaluation of fracture trace maps from rock tunnel face images via deep learning. *International Journal of Rock Mechanics and Mining Sciences*, 142, 104745.
- Chen, G., Ruan, B., Zhao, K., Chen, W., Zhuang, H., Du, X., Khoshnevisan, S., & Juang, C. H. (2020). Nonlinear response characteristics of undersea shield tunnel subjected to strong earthquake motions. *Journal of Earthquake Engineering*, 24(3), 351–380.
- Chen, Z., & Wei, J. (2013). Correlation between ground motion parameters and lining damage indices for mountain tunnels. *Natural Hazards*, 65(3), 1683–1702.
- Chern, S., Tsai, J. H., Chien, L. K., & Huang, C. Y. (2009). Predicting lateral wall deflection in top-down excavation by neural network. *International Journal of Offshore and Polar Engineering*, 19(2), 151–157.
- Corigliano, M., Lai, C. G., & Barla, G. (2007). Seismic vulnerability of rock tunnels using fragility curves. Paper presented at the 11th ISRM

- Congress, Lisbon, Portugal, July 2007. ISRM-11CONGRESS-2007-257.
- de Silva, F., Fabozzi, S., Nikitas, N., Bilotta, E., & Fuentes, R. (2021). Seismic vulnerability of circular tunnels in sand. *Géotechnique*, 1–15.
- Gardoni, P., Mosalam, K. M., & Der Kiureghian, A. (2003). Probabilistic seismic demand models and fragility estimates for RC bridges. *Journal of Earthquake Engineering*, 7(spec01), 79–106.
- GB50011—2010 (2010). *Code for seismic design of buildings*. Beijing, China: China Architecture and Building Press (in Chinese).
- Hashash, Y. M., Hook, J. J., Schmidt, B., John, I., & Yao, C. (2001). Seismic design and analysis of underground structures. *Tunnelling and Underground Space Technology*, 16(4), 247–293.
- Hassoun, M. H. (1995). *Fundamentals of artificial neural networks*. MIT Press.
- Hatzigeorgiou, G. D., & Beskos, D. E. (2010). Soil–structure interaction effects on seismic inelastic analysis of 3-D tunnels. *Soil Dynamics and Earthquake Engineering*, 30(9), 851–861.
- Haykin, S. (2010). *Neural networks: A comprehensive foundation*. 1999. Mc Millan, New Jersey, pp. 1–24.
- Hu, X., Zhou, Z., Chen, H., & Ren, Y. (2020). Seismic fragility analysis of tunnels with different buried depths in a soft soil. *Sustainability*, 12(3), 892.
- Huang, H. W., & Zhang, D. M. (2016). Resilience analysis of shield tunnel lining under extreme surcharge: Characterization and field application. *Tunnelling and Underground Space Technology*, 51, 301–312.
- Huang, Z. K., Ptilakis, K., Argyroudis, S., Tsinidis, G., & Zhang, D. M. (2021). Selection of optimal intensity measures for fragility assessment of circular tunnels in soft soil deposits. *Soil Dynamics and Earthquake Engineering*, 145, 106724.
- Huang, Z. K., Ptilakis, K., Tsinidis, G., Argyroudis, S., & Zhang, D. M. (2020). Seismic vulnerability of circular tunnels in soft soil deposits: The case of Shanghai metropolitan system. *Tunnelling and Underground Space Technology*, 98, 103341.
- Iervolino, I., & Manfredi, G. (2008). A review of ground motion record selection strategies for dynamic structural analysis. *Modern Testing Techniques for Structural Systems*, 131–163.
- Jalayer, F., De Risi, R., & Manfredi, G. (2015). Bayesian Cloud Analysis: Efficient structural fragility assessment using linear regression. *Bulletin of Earthquake Engineering*, 13(4), 1183–1203.
- Jin, Y. F., Zhu, B. Q., Yin, Z. Y., & Zhang, D. M. (2019). Three-dimensional numerical analysis of the interaction of two crossing tunnels in soft clay. *Underground Space*, 4(4), 310–327.
- Karafagka, S., Fotopoulou, S., & Ptilakis, D. (2021). Fragility curves of non-ductile RC frame buildings on saturated soils including liquefaction effects and soil–structure interaction. *Bulletin of Earthquake Engineering*, 1–26.
- Khosravikia, F., Kurkowski, J., & Clayton, P. (2020). Fragility of masonry veneers to human-induced Central US earthquakes using neural network models. *Journal of Building Engineering*, 28, 101100.
- Lagaros, N. D., Tsompanakis, Y., Psarropoulos, P. N., & Georgopoulos, E. C. (2009). Computationally efficient seismic fragility analysis of geostructures. *Computers & Structures*, 87(19–20), 1195–1203.
- Liu, T., Chen, Z., Yuan, Y., & Shao, X. (2017). Fragility analysis of a subway station structure by incremental dynamic analysis. *Advances in Structural Engineering*, 20(7), 1111–1124.
- Liu, Z., & Zhang, Z. (2018). Artificial neural network based method for seismic fragility analysis of steel frames. *KSCE Journal of Civil Engineering*, 22(2), 708–717.
- Lysmer, J., & Kuhlemeyer, R. L. (1969). Finite dynamic model for infinite media. *Journal of the Engineering Mechanics Division*, 95(4), 859–877.
- Mangalathu, S., Heo, G., & Jeon, J. S. (2018). Artificial neural network based multi-dimensional fragility development of skewed concrete bridge classes. *Engineering Structures*, 162, 166–176.
- Marquardt, D. W. (1963). An algorithm for least-squares estimation of nonlinear parameters. *Journal of the Society for Industrial and Applied Mathematics*, 11(2), 431–441.
- MathWorks (2018). *Global optimization toolbox: User's Guide (R2018)*.
- Mitropoulou, C. C., & Papadrakakis, M. (2011). Developing fragility curves based on neural network IDA predictions. *Engineering Structures*, 33(12), 3409–3421.
- Nguyen, D. D., Park, D., Shamsher, S., Nguyen, V. Q., & Lee, T. H. (2019). Seismic vulnerability assessment of rectangular cut-and-cover subway tunnels. *Tunnelling and Underground Space Technology*, 86, 247–261.
- Pacific Earthquake Engineering Research Center (PEER) (2000). *PEER strong motion database*. Berkeley, CA: University of California, Berkeley.
- Ptilakis, K., Alexoudi, M., Argyroudis, S., Monge, O., & Martin, C. (2006). Earthquake risk assessment of lifelines. *Bulletin of Earthquake Engineering*, 4(4), 365–390.
- Ptilakis, K., & Tsinidis, G. (2014). Performance and seismic design of underground structures. In *Earthquake geotechnical engineering design* (pp. 279–340). Cham: Springer.
- Ranasinghe, R. A. T. M., Jaksa, M. B., Kuo, Y. L., & Nejad, F. P. (2017). Application of artificial neural networks for predicting the impact of rolling dynamic compaction using dynamic cone penetrometer test results. *Journal of Rock Mechanics and Geotechnical Engineering*, 9(2), 340–349.
- Salsani, A., Daneshian, J., Shariati, S., Yazdani, C. A., & Taheri, M. (2014). Predicting roadheader performance by using artificial neural network. *Neural Computing and Applications*, 24(7), 1823–1831.
- Sayed, M. A., Kwon, O. S., Park, D., & Van Nguyen, Q. (2019). Multi-platform soil–structure interaction simulation of Daikai subway tunnel during the 1995 Kobe earthquake. *Soil Dynamics and Earthquake Engineering*, 125, 105643.
- Shahin, M. A., Jaksa, M. B., & Maier, H. R. (2001). Artificial neural network applications in geotechnical engineering. *Australian Geomechanics*, 36(1), 49–62.
- Shokri, M., & Tavakoli, K. (2019). A review on the artificial neural network approach to analysis and prediction of seismic damage in infrastructure. *International Journal of Hydromechanics*, 2(4), 178–196.
- Tsinidis, G., Ptilakis, K., Madabhushi, G., & Heron, C. (2015). Dynamic response of flexible square tunnels: Centrifuge testing and validation of existing design methodologies. *Géotechnique*, 65(5), 401–417.
- Tsinidis, G., Rovithis, E., Ptilakis, K., & Chazelas, J. L. (2016). Seismic response of box-type tunnels in soft soil: Experimental and numerical investigation. *Tunnelling and Underground Space Technology*, 59, 199–214.
- Tsinidis, G., de Silva, F., Anastasopoulos, I., Bilotta, E., Bobet, A., Hashash, Y. M., He, C., Kampas, G., Knappett, J., Madabhushi, G., & Nikitas, N. (2020). Seismic behaviour of tunnels: From experiments to analysis. *Tunnelling and Underground Space Technology*, 99, 103334.
- Tsinidis, G., Ptilakis, K., & Trikalioti, A. D. (2014). Numerical simulation of round robin numerical test on tunnels using a simplified kinematic hardening model. *Acta Geotechnica*, 9(4), 641–659.
- Vamvatsikos, D., & Cornell, C. A. (2002). Incremental dynamic analysis. *Earthquake Engineering & Structural Dynamics*, 31(3), 491–514.
- Wang, T. T., Kwok, O. L. A., & Jeng, F. S. (2021). Seismic response of tunnels revealed in two decades following the 1999 Chi-Chi earthquake (Mw 7.6) in Taiwan: A review. *Engineering Geology*, 287, 106090.
- Wang, Z., Pedroni, N., Zentner, I., & Zio, E. (2018). Seismic fragility analysis with artificial neural networks: Application to nuclear power plant equipment. *Engineering Structures*, 162, 213–225.
- Yu, H., Chen, J., Bobet, A., & Yuan, Y. (2016). Damage observation and assessment of the Longxi tunnel during the Wenchuan earthquake. *Tunnelling and Underground Space Technology*, 54, 102–116.
- Zhang, W., Li, H., Li, Y., Liu, H., Chen, Y., & Ding, X. (2021). Application of deep learning algorithms in geotechnical engineering: A short critical review. *Artificial Intelligence Review*, 1–41.
- Zhang, W. G., Li, H. R., Wu, C. Z., Li, Y. Q., Liu, Z. Q., & Liu, H. L. (2021). Soft computing approach for prediction of surface settlement induced by earth pressure balance shield tunneling. *Underground Space*, 6(4), 353–363.
- Zheng, G., Zhang, W., Zhang, W., Zhou, H., & Yang, P. (2021). Neural network and support vector machine models for the prediction of the liquefaction-induced uplift displacement of tunnels. *Underground Space*, 6(2), 126–133.
- Zhong, Z., Shen, Y., Zhao, M., Li, L., Du, X., & Hao, H. (2020). Seismic fragility assessment of the Daikai subway station in layered soil. *Soil Dynamics and Earthquake Engineering*, 132, 106044.
- Zi, H., Ding, Z., Ji, X., Liu, Z., & Shi, C. (2021). Effect of voids on the seismic vulnerability of mountain tunnels. *Soil Dynamics and Earthquake Engineering*, 148, 106833.